

## Article

# Soil Treatment to Reduce Grounding Resistance by Applying Low-Resistivity Material (LRM) Implemented in Different Grounding Systems Configurations and in Soils with Different Resistivities

Freddy Sinchi-Sinchi <sup>†</sup>, Cristian Coronel-Naranjo <sup>†</sup>, Antonio Barragán-Escandón <sup>\*</sup>  
and Flavio Quizhpi-Palomeque <sup>\*</sup>

Energy Research Group (GIE), Electrical Engineering Career, Salesian Polytechnic University (Universidad Politécnica Salesiana—UPS), Cuenca EC010105, Ecuador; fsinchi@est.ups.edu.ec (F.S.-S.); ccoronel@est.ups.edu.ec (C.C.-N.)

<sup>\*</sup> Correspondence: ebarragan@ups.edu.ec (A.B.-E.); fquizhpi@ups.edu.ec (F.Q.-P.)

<sup>†</sup> These authors contributed equally to this work.

**Abstract:** In the present study, field tests were performed using low-resistivity materials (LRMs) in different grounding system (GS) configurations to reduce the grounding resistance (GR) and assess the variation in the effectiveness of the LRMs with increases in the complexity of the GS design. Different configurations were implemented in soils with different resistivity values to determine the variation in the effectiveness of each LRM design with increases in the soil resistivity. Lastly, the percentage decrease in the GR was assessed as a function of the increase in the complexity of the GS design and the variation in the soil resistivity. The results of this study provide a useful guide for engineers and researchers who study, design, and build innovative and effective GSs by applying improved compounds for safe electrical installations.

**Keywords:** soil resistivity; low-resistivity material (LRM); grounding systems; grounding resistance



**Citation:** Sinchi-Sinchi, F.; Coronel-Naranjo, C.; Barragán-Escandón, A.; Quizhpi-Palomeque, F. Soil Treatment to Reduce Grounding Resistance by Applying Low-Resistivity Material (LRM) Implemented in Different Grounding Systems Configurations and in Soils with Different Resistivities. *Appl. Sci.* **2022**, *12*, 4788. <https://doi.org/10.3390/app12094788>

Academic Editor: Gian Giuseppe Soma

Received: 22 March 2022

Accepted: 4 May 2022

Published: 9 May 2022

**Publisher's Note:** MDPI stays neutral with regard to jurisdictional claims in published maps and institutional affiliations.



**Copyright:** © 2022 by the authors. Licensee MDPI, Basel, Switzerland. This article is an open access article distributed under the terms and conditions of the Creative Commons Attribution (CC BY) license (<https://creativecommons.org/licenses/by/4.0/>).

## 1. Introduction

Grounding systems (GSs) are an integral part of electrical power systems (transmission and distribution facilities). They ensure the safety of personnel and equipment by protecting against fault currents caused by lightning, device failure, or surges. Therefore, an effective GS is needed to effectively and safely discharge fault currents to the ground [1].

In Ecuador, a lack of standards has prevented the implementation of configurations that consider specific variables and ensure the adequate operation of GSs. The variables that influence the design of GSs include the soil resistivity, the rod length and radius, the ground conductor [2] and the burial depth. Another key parameter that is often overlooked is the lack of soil uniformity. For example, soils with more than one layer are considered to have a uniform resistivity, which therefore affects the design of equipment and the protection conditions. All of these factors may lead to designs that are either oversized or fail to meet the required soil resistivity needs [2].

The grounding resistance (GR) is usually reduced to desired values by increasing the number of horizontal (grid) conductors or rods. However, this procedure or “physical reduction” does not always make it possible to achieve this objective. Alternatively, the radius of the ground electrode can be increased, and the surrounding soil can be modified with low-resistivity materials (LRMs) (chemical reduction) [3–5].

The commonly used formulation of the Institute of Electrical and Electronics Engineers (IEEE) standard 80-2013 [3] for the design of GSs requires exhaustive calculations and may lead to an infinite number of designs. However, the standard also states the following: “While the grounding systems may be adjusted to eliminate dangerous contact potentials

by suppression of ground short-circuit currents, this is not usually demanded solidly grounded neutral systems because it does not appear to be practicable. For ground fault currents above 1000 A, grounding systems of vast dimensions must be installed in order to meet the usual 125 V contact potential requirement". The grounding configurations of this study are designed for fault currents less than 1000 A.

This article presents the results from field tests based on a combination of calculations and measurements and the use of LRMs available in the local market. The results show that the GR can be considerably reduced by using such materials in simple configurations and in high-resistivity soils.

## 2. Theoretical Framework

### 2.1. Grounding Systems

GSs are present in almost all points of the electrical grid, including power stations and transmission lines and cables, which distribute electrical energy.

The primary function of a GS is to provide various routes to drive electrical currents to the ground or to establish contact with the ground without exceeding the limits of any operating equipment, thereby preventing service interruptions.

Using a GS with various shapes and geometries ensures the safety of people and the reliable operation of electrical equipment. Researchers have proposed various ways to identify optimal GS designs, such as the approach proposed by [6]. These authors performed a comparative analysis of three grounding grid configurations in a two-layer soil model. After designing equally and unequally spaced grounding grids for each shape, they found that the unequally spaced rectangular grid outperformed the other designs. The study showed that the rectangular grid had the minimum GR value.

### 2.2. Soil Resistivity

To calculate and design a GS, the soil resistivity in the desired location of the connection must be investigated to determine the general composition and degree of uniformity of the soil. Several tables of the resistivity ranges for various soils and rocks are available in the engineering literature, such as those found in [3,7–10]. However, resistivity should not be estimated based on soil classification because these tables provide only approximate values. Accordingly, resistivity tests must be performed [3,11].

### 2.3. Grounding Resistance

The GR is considered to be the main factor in determining the geometry of any GS because this parameter measures how much the ground resists the fault current flow [5,12].

Developing a low-resistance ground electrode is a fundamental requirement to meet the demands of power distribution feeders because the fault return path is through the ground. The operability requirements of systems can be met more easily for lower GR values.

IEEE standard 80-2013 [3] recommend using simple empirical equations to analyse GS parameters. These equations are derived based on an approximate treatment of GSs using theoretical analyses, numerical calculations, and simulation tests [7].

### 2.4. Soil Treatment for Grounding Resistance Reduction

Various methods and materials have been proposed for mitigating the problem of high soil resistivity and GR values [13]. Several studies, including [1,4,5,12–20], have been conducted to provide LRMs with specific characteristics to further improve the performance of GSs, for example, by improving the ability to retain moisture in the soil near the ground rod, by decreasing the surrounding soil resistivity, and by creating a protective layer to prevent ground rod corrosion [15]. Therefore, an improved material suitable for GSs must be selected, depending on the soil type and local climate [12].

Currently, bentonite is widely used as an LRM and recommended in IEEE standard 80-2013 [3]. Bentonite can absorb up to five times its weight in water. In addi-

tion, its dry volume can be increased by up to 13 times, and it can adhere to almost any surface [1,5,15,17,18,21].

As reviewed by [1], bentonite perform well as an LRM in the presence of water, with a decrease in resistivity of up to 60%. Bentonite is a chemically inert material and, therefore, a noncorrosive agent for metal electrodes.

In [15], the behaviour of bentonite was analysed on three different sites. The authors concluded that this LRM performed best in soils with a greater resistivity. In addition, they determined that the GR fluctuated over the year of testing on all rods due to seasonal variations.

### 3. Experimental Research

In this project, the deductive method was used to move from general to specific research questions [22]. The project was divided into the following steps.

#### 3.1. Step 1: Data Collection

In the first phase of the project, data were collected [23]; more specifically, the soil resistivity was measured using a tellurometer. The resistivity values ranged from 1  $\Omega\cdot\text{m}$  to 302  $\Omega\cdot\text{m}$  in the field tests at different soil resistivity values using the same GS configurations.

#### 3.2. Step 2: Soil Modelling

After measuring the apparent resistivity of the soils in step 1, each soil was modelled to assess its resistivity by using the uniform soil model for moderate variations and the two-layer soil model for marked variations in resistivity with depth, according to IEEE standard 80-2013 [3].

#### 3.3. Step 3: Implementation of GS Designs

In the third phase of the project, several GS configurations were implemented in the study soils (see Figure 1). The configurations were limited to three rods in soils 1, 2, 3, 4, 7 and 8 and six rods in soils 5 and 6. In addition, these configurations were chosen because measured GR values can be compared to calculations using equations previously developed and published in the literature [3,24,25].

The code of each configuration is detailed below:

- 1R: One vertical rod.
- 2RP: Two rods connected in a parallel grid.
- 3RP: Three rods connected in a parallel grid.
- 3RT: Three rods connected in a triangular grid.
- 6RR: Six rods connected in a rectangular grid.

For each configuration, copper rods with a length ( $L_r$ ) of 1.80 m  $\times$  5/8" and spaced at a distance ( $d$ ) of 3.80 m were used. The #4 AWG stranded bare copper conductor was buried at a depth ( $h$ ) of 0.25 m.

#### 3.4. Step 4: GR Calculations

The GR of each GS design was calculated using the equations found in [24] for the 1R configuration, the equations reported in [25] for the 2RP, 3RP and 3RT configurations, and the equations found in IEEE standard 80-2013 [3] for the 6RR configuration.

##### 3.4.1. Earth Resistance of a Rod

The GR for the configuration of a rod in a vertical arrangement (see configuration 1R of Figure 1) can be calculated using Equation (1) developed by Dwight [24].

$$R = \frac{\rho}{2\pi L_r} \left( \ln \frac{4L_r}{b} - 1 \right) \quad (1)$$

where:  
 $\rho$ : ground resistivity, [ $\Omega \cdot m$ ]  
 $L_r$ : rod length, [m]  
 $b$ : rod radius, [m]

| Configuration code | Schematic representation | Soil   |
|--------------------|--------------------------|--|
| 1R                 |                          | Soil 1<br>Soil 2<br>Soil 3<br>Soil 4<br>Soil 7<br>Soil 8 |
| 2RP                |                          | Soil 1<br>Soil 2<br>Soil 3<br>Soil 4<br>Soil 7<br>Soil 8 |
| 3RP                |                          | Soil 1<br>Soil 2<br>Soil 3<br>Soil 4<br>Soil 7<br>Soil 8 |
| 3RT                |                          | Soil 1<br>Soil 2<br>Soil 3<br>Soil 4<br>Soil 7<br>Soil 8 |
| 6RR                |                          | Soil 5<br>Soil 6   |

Figure 1. Basic GS configurations applied in each soil.

### 3.4.2. Ground Resistance of Two Rod Connection

The calculation of the GR for two and three bars developed in [25], unlike the Dwight equations, considers the effect of the GR of the conductor.

The GR of two rods (see configuration 2RP of Figure 1) is calculated by Equation (2).  $R_1$ ,  $R_2$  and  $R_m$  and  $R_m$  are obtained by Equations (3), (4) and (5), respectively.

$$R_g = \frac{R_1 R_2 - R_m^2}{R_1 + R_2 - 2R_m} \tag{2}$$

$$R_1 = \frac{\rho}{\pi d} \left[ \ln \left( \frac{2d}{a'} \right) + 4k_1 - k_2 \right] \tag{3}$$

$$R_2 = \frac{\rho}{4\pi L_r} \left[ \ln \left( \frac{4L_r}{b} \right) - 1 + \frac{8k_1 \times L_r}{d} (\sqrt{2} - 1)^2 \right] \tag{4}$$

$$R_m = R_1 - \frac{\rho}{\pi d} \left[ \ln \left( \frac{L_r}{\sqrt{h \times 2a}} \right) - 1 \right] \tag{5}$$

where:

$\rho$ : ground resistivity, [ $\Omega \cdot m$ ]

$L_r$ : rod length, [m]

$b$ : rod radius, [m]

$R_1$ : resistance to earth of the conductor, [ $\Omega$ ]

$R_2$ : earth resistance of the rods, [ $\Omega$ ]

$R_m$ : mutual resistance between mesh and rods, [ $\Omega$ ]

$R_g$ : overall system resistance, [ $\Omega$ ]

$d$ : separation distance between two rods,  $d > L_r$ , [m]

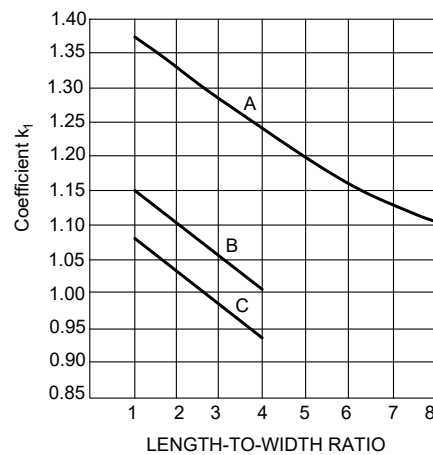
$h$ : conductor burial depth, [m]

$a$ : conductor radius, [m]

$a'$ : is  $a$  for the conductor on the surface of the earth, [m] or

$a'$ : is  $\sqrt{a} \cdot 2h$  for conductors buried at a depth  $h$ , [m]

$k_1$  and  $k_2$ : coefficients [see Figures 2 and 3, respectively]



CURVE A - FOR DEPTH  $h = 0$   
 $y_A = -0.04x + 1.41$   
 CURVE B - FOR DEPTH  $h = 1/10 \cdot \sqrt{\text{AREA}}$   
 $y_B = -0.05x + 1.20$   
 CURVE C - FOR DEPTH  $h = 1/6 \cdot \sqrt{\text{AREA}}$   
 $y_C = -0.05x + 1.13$

Figure 2. Coefficient  $k_1$ .

For the process of calculating the GR of the present study, Equations (6) and (7) are used obtained from curves B of Figures 2 and 3 for  $k_1$  and  $k_2$ , respectively.

$$k_1 = -0.05 \left( \frac{L_x}{L_y} \right) + 1.20 \tag{6}$$

$$k_2 = 0.10 \left( \frac{L_x}{L_y} \right) + 4.68 \tag{7}$$

where:

$k_1$  and  $k_2$ : are the coefficients

$L_x$ : maximum length of braided conductors in  $x$ , long, [m]

$L_y$ : maximum length of mesh conductors in  $y$ , width, [m]

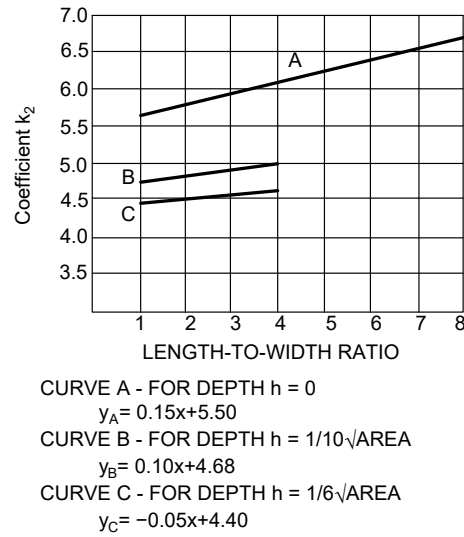


Figure 3. Coefficient  $k_2$ .

According to [25],  $x = 1$  for the configurations of two linearly connected rods (Section 3.4.2), three linearly connected rods (Section 3.4.3), and three triangularly connected rods (Section 3.4.4).

### 3.4.3. Resistance to Earth of the Connection of Three Rods in Line

The total GR of the system for the configurations of three rods in a linear arrangement (see configuration 3RP of Figure 1) is obtained by means of Equation (2). In this case,  $R_1$ ,  $R_2$  and  $R_m$  are established by Equations (8), (9) and (10), respectively.

$$R_1 = \frac{\rho}{2\pi d} \left[ \ln \left( \frac{4d}{a'} \right) + 4k_1 - k_2 \right] \tag{8}$$

$$R_2 = \frac{\rho}{6\pi L_r} \left[ \ln \left( \frac{4L_r}{b} \right) - 1 + \frac{4k_1 \times L_r}{d} (\sqrt{3} - 1)^2 \right] \tag{9}$$

$$R_m = R_1 - \frac{\rho}{2\pi d} \left[ \ln \left( \frac{L_r}{\sqrt{h \times 2a}} \right) - 1 \right] \tag{10}$$

where:

$\rho$ : ground resistivity, [ $\Omega \cdot m$ ]

$L_r$ : rod length, [m]

$b$ : rod radius, [m]

$R_1$ : resistance to earth of the conductor, [ $\Omega$ ]

$R_2$ : earth resistance of the rods, [ $\Omega$ ]

$R_m$ : mutual resistance between mesh and rods, [ $\Omega$ ]

$d$ : separation distance between two rods,  $d > L_r$ , [m]

$h$ : conductor burial depth, [m]

$a$ : conductor radius, [m]

$a'$ : is  $a$  for the conductor on the surface of the earth, [m] or

$a'$ : is  $\sqrt{a \cdot 2h}$  for conductors buried at a depth  $h$ , [m]

$k_1$  and  $k_2$ : coefficients [see Figures 2 and 3, respectively]

### 3.4.4. Earth Resistance of a Triangular Mesh

The GR of the triangular mesh (see 3RT configuration of Figure 1) is calculated using EQUATION (2), where  $R_1$ ,  $R_2$  and  $R_m$  are defined with Equations (11), (12) and (13), respectively.

$$R_1 = \frac{\rho}{3\pi d} \left[ \ln \left( \frac{6d}{a'} \right) + \frac{3k_1 \times d}{\sqrt{A}} - k_2 \right] \quad (11)$$

$$R_2 = \frac{\rho}{6\pi L_r} \left[ \ln \left( \frac{4L_r}{b} \right) - 1 + \frac{2k_1 \times L_r}{\sqrt{A}} (\sqrt{3} - 1)^2 \right] \quad (12)$$

$$R_m = R_1 - \frac{\rho}{3\pi d} \left[ \ln \left( \frac{L_r}{\sqrt{h \times 2a}} \right) - 1 \right] \quad (13)$$

where:

$\rho$ : ground resistivity, [ $\Omega \cdot \text{m}$ ]

$L_r$ : rod length, [m]

$b$ : rod radius, [m]

$R_1$ : resistance to earth of the conductor, [ $\Omega$ ]

$R_2$ : earth resistance of the rods, [ $\Omega$ ]

$R_m$ : mutual resistance between mesh and rods, [ $\Omega$ ]

$d$ : separation distance between two rods,  $d > L_r$ , [m]

$h$ : conductor burial depth, [m]

$a$ : conductor radius, [m]

$a'$ : is  $a$  for the conductor on the surface of the earth, [m] or

$a'$ : is  $\sqrt{a} \cdot 2h$  for conductors buried at a depth  $h$ , [m]

$k_1$  and  $k_2$ : coefficients [see Figures 2 and 3, respectively]

$A$ : is the area covered by the conductors, [ $\text{m}^2$ ]

### 3.4.5. Earth Resistance of Square and Rectangular Meshes

The calculation of the GR of the rectangular mesh with 6RR configuration of Figure 1 is calculated through the Schwarz equations. The total resistance ( $R_g$ ) for a uniform soil containing conductors and rods is calculated using Equation (2). While  $R_1$ ,  $R_2$  and  $R_m$  are defined with Equations (14), (15) and (16), respectively. The coefficients  $k_1$  and  $k_2$  are obtained from Figures 2 and 3, respectively.

$$R_1 = \frac{\rho}{\pi L_c} \left[ \ln \left( \frac{2L_c}{a'} \right) + \frac{k_1 \times L_c}{\sqrt{A}} - k_2 \right] \quad (14)$$

$$R_2 = \frac{\rho}{2\pi n_R L_r} \left[ \ln \left( \frac{4L_r}{b} \right) - 1 + \frac{2k_1 \times L_r}{\sqrt{A}} (\sqrt{n_R} - 1)^2 \right] \quad (15)$$

$$R_m = \frac{\rho}{\pi L_c} \left[ \ln \left( \frac{2L_c}{L_r} \right) + \frac{k_1 \times L_c}{\sqrt{A}} - k_2 + 1 \right] \quad (16)$$

Equation (16) can also be written as Equation (17).

$$R_m = R_1 - \frac{\rho}{\pi L_c} \left[ \ln \left( \frac{L_r}{\sqrt{h \times 2a}} \right) - 1 \right] \quad (17)$$

where:

$\rho$ : ground resistivity, [ $\Omega \cdot \text{m}$ ]

$L_r$ : rod length, [m]

$b$ : rod radius, [m]

$R_1$ : resistance to earth of the conductor, [ $\Omega$ ]

$R_2$ : earth resistance of the rods, [ $\Omega$ ]

$R_m$ : mutual resistance between mesh and rods, [ $\Omega$ ]

$d$ : separation distance between two rods,  $d > L_r$ , [m]

$h$ : conductor burial depth, [m]

$a$ : conductor radius, [m]

$a'$ : is  $a$  for the conductor on the surface of the earth, [m] or

$a'$ : is  $\sqrt{a} \cdot 2h$  for conductors buried at a depth  $h$ , [m]

$k_1$  and  $k_2$ : coefficients [see Figures 2 and 3, respectively]  
 $L_c$ : total length of the conductors connected to the mesh, [m]  
 $A$ : is the area covered by the conductors, [m<sup>2</sup>]  
 $n_R$ : number of rods located in the area  $A$

### 3.5. Step 5: GR Measurements

The GR was measured using fall-of-potential methods and the clamp-on or stakeless method described in IEEE standard 81-2012 [26] and subsequently compared with theoretical calculations.

### 3.6. Step 6: LRM Implementation

The chemical treatment for reducing soil resistivity consists of adding an LRM to the local soil near the electrode to improve the electrical conductivity of the soil and thus reduce the GR. According to [7], the construction methods for grounding devices with different structures in soils with different resistivities can be classified into three categories: filling, penetration, and trench methods.

In the present project, premixed and dry LRMs were used [5]. The materials were implemented by applying the filling method, which is commonly used to build a vertical ground rod.

The vertical rods of the GS configurations presented in step 3 were covered with the LRM. Figure 4 shows the configuration code, a schematic representation of each configuration covered with the LRM and the soils where each design was located.

The code of each configuration is detailed below:

- 1LRMR: One vertical rod with LRM.
- 2LRMRP: Two rods with LRM connected in a parallel grid.
- 3LRMRP: Three rods with LRM connected in a parallel grid.
- 3LRMRT: Three rods with LRM connected in a triangular grid.
- 6LRMRR: Six rods with LRM connected in a rectangular grid.

### 3.7. Step 7: Measurement of the GR

The GR was again measured using the fall-of-potential and clamp-on or stakeless methods described in IEEE standard 81-2012 [26] to subsequently analyse the results and determine the variation in the percentage effectiveness of the LRM as the ground resistivity and complexity of the GS increased.

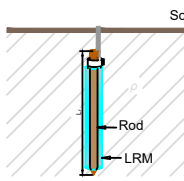
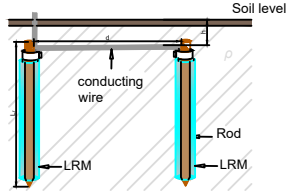
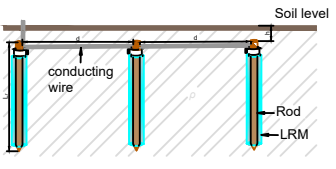
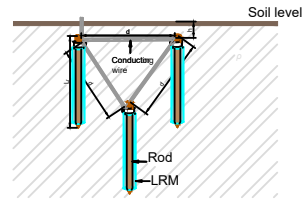
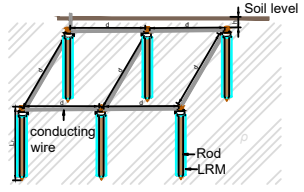
| Configuration code | Schematic representation   | Soil   |
|--------------------|--|--|
| 1LRMR              |    | Soil 1<br>Soil 2<br>Soil 3<br>Soil 4<br>Soil 7<br>Soil 8 |
| 2LRMRP             |    | Soil 1<br>Soil 2<br>Soil 3<br>Soil 4<br>Soil 7<br>Soil 8 |
| 3LRMRP             |    | Soil 1<br>Soil 2<br>Soil 3<br>Soil 4<br>Soil 7<br>Soil 8 |
| 3LRMRT             |   | Soil 1<br>Soil 2<br>Soil 3<br>Soil 4<br>Soil 7<br>Soil 8 |
| 6LRMRR             |  | Soil 5<br>Soil 6   |

Figure 4. Basic GS designs with LRM.

#### 4. Results

##### 4.1. Results of Resistivity Measurements

The field tests were conducted in rural areas with large green areas using GS elements. In the canton Cuenca, studies involving direct soil resistivity measurements have been conducted by [27–29], and the reported values are outlined in Table 1.

Table 1. Resistivity values measured in the canton Cuenca.

| Measured Resistivity ( $\Omega \cdot m$ ) |        |        |        |        |        |        |        |        |
|---|--------|--------|--------|--------|--------|--------|--------|--------|
| 5.48                                      | 11.53  | 13.02  | 13.17  | 13.45  | 13.61  | 13.95  | 14.05  | 14.16  |
| 14.87                                     | 14.88  | 14.99  | 15.63  | 15.94  | 16.24  | 16.34  | 16.41  | 16.91  |
| 17.06                                     | 17.12  | 17.18  | 19.49  | 19.86  | 23.80  | 24.10  | 27.10  | 29.40  |
| 49.54                                     | 103.16 | 104.34 | 106.41 | 110.68 | 120.28 | 144.05 | 202.12 | 247.57 |

The resistivity was measured in eight soils using the Wenner method (see Figure 5). This method is suitable according to IEEE standard 81-2012 [26].



**Figure 5.** Measurement of the soil resistivity 1 (S1).

The spacings between the stakes for each measurement selected for the Wenner method were 1, 2 and 3 m. The measurements were performed in four directions ( $0^\circ$ ,  $45^\circ$ ,  $90^\circ$  and  $135^\circ$ ), as shown in Figure 6.

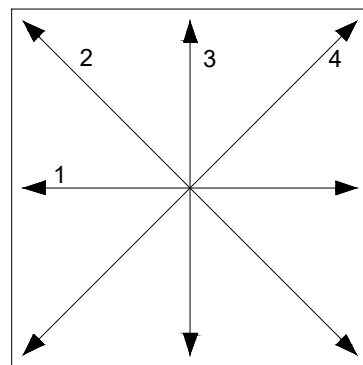


**Figure 6.** Directions of the resistivity measurement.

#### 4.2. Soil Modelling Results

The results of the measurements were interpreted in uniform soil models using Sunde's graphical method according to IEEE standard 80-2013 [3]. Table 2 summarises the soil resistivity values of the eight soils. According to [9], a uniform soil model can be used when the measured soil resistivity values are within  $\pm 30\%$  of the arithmetic mean; otherwise, a two-layer soil model should be used.

**Table 2.** Modelled resistivity of each soil.

| Soil | Resistivity ( $\Omega \cdot m$ ) | Model                    | Variation |
|------|----------------------------------|--------------------------|-----------|
| S1   | 23.30 $\approx$ 24               | Uniform soil             | 25%       |
| S2   | 34.96 $\approx$ 35               | Sunde's graphical method | 45%       |
| S3   | 151.73 $\approx$ 152             | Sunde's graphical method | 40%       |
| S4   | 158.08 $\approx$ 159             | Sunde's graphical method | 45%       |
| S5   | 174.12 $\approx$ 175             | Sunde's graphical method | 38%       |
| S6   | 189.37 $\approx$ 190             | Sunde's graphical method | 31%       |
| S7   | 194.37 $\approx$ 195             | Sunde's graphical method | 41%       |
| S8   | 301.55 $\approx$ 302             | Sunde's graphical method | 49%       |

#### 4.3. Results of GR Calculations and Measurements

The GR of each implemented design was measured using the fall-of-potential (see Figure 7a) and clamp-on or stakeless (see Figure 7b) methods. The latter was applied to compare the readings obtained using the former. The GR values assessed using the fall-of-potential (FOP) method were recorded for subsequent analysis.



(a)



(b)

**Figure 7.** Grounding resistance (GR) measurements. (a) FOP method; (b) Clamp-on method.

Table 3 outlines the calculated and measured GR values of the GSs implemented in soil 1 (S1), for which the resistivity was 24  $\Omega$ -m. The premixed LRM (P) was used in this soil.

**Table 3.** GR calculations and measurements in S1.

| Configuration Code | Calculated Grounding Resistance ( $\Omega$ ) | Measured Grounding Resistance         |                              |
|--------------------|--|---------------------------------------|------------------------------|
|                    |  | Fall-of-Potential Method ( $\Omega$ ) | Clamp-on Method ( $\Omega$ ) |
| 1R                 | 12.31  | 12.40                                 | 13.27                        |
| 2RP                | 6.24   | 6.84                                  | 8.01                         |
| 3RP                | 4.13   | 5.06                                  | 6.48                         |
| 3RT                | 3.67   | 4.80                                  | 6.07                         |
| 1LRMR P            | —  | 7.06                                  | 7.81                         |
| 2LRMRP P           | —  | 5.03                                  | 5.56                         |
| 3LRMRP P           | —  | 3.82                                  | 4.47                         |
| 3LRMRT P           | —  | 3.80                                  | 4.44                         |

Table 4 outlines the calculated and measured GR values of the GSs implemented in soil 2 (S2), for which the resistivity was 35  $\Omega$ -m. The dry LRM (D) was used in this soil.

**Table 4.** GR calculations and measurements in S2.

| Configuration Code | Calculated Grounding Resistance ( $\Omega$ ) | Measured Grounding Resistance         |                              |
|--------------------|--|---------------------------------------|------------------------------|
|                    |  | Fall-of-Potential Method ( $\Omega$ ) | Clamp-on Method ( $\Omega$ ) |
| 1R                 | 17.96  | 24.03                                 | 19.59                        |
| 2RP                | 9.10   | 9.13                                  | 9.70                         |
| 3RP                | 6.03   | 5.81                                  | 6.60                         |
| 3RT                | 5.35   | 5.50                                  | 6.63                         |
| 1LRMR D            | —  | 15.46                                 | 15.78                        |
| 2LRMRP D           | —  | 7.85                                  | 8.54                         |
| 3LRMRP D           | —  | 5.72                                  | 6.22                         |
| 3LRMRT D           | —  | 5.42                                  | 6.22                         |

Table 5 outlines the calculated and measured GR values of the GSs implemented in soil 3 (S3), for which the resistivity was 153  $\Omega$ ·m. The premixed LRM (P) was used in this soil.

**Table 5.** GR calculations and measurements in S3.

| Configuration Code | Calculated Grounding Resistance ( $\Omega$ ) | Measured Grounding Resistance         |                              |
|--------------------|--|---------------------------------------|------------------------------|
|                    |  | Fall-of-Potential Method ( $\Omega$ ) | Clamp-on Method ( $\Omega$ ) |
| 1R                 | 77.98  | 72.60                                 | 66.10                        |
| 2RP                | 39.51  | 36.42                                 | 35.80                        |
| 3RP                | 26.18  | 26.00                                 | 26.20                        |
| 3RT                | 23.25  | 22.50                                 | 22.10                        |
| 1LRMR P            | —  | 33.85                                 | 33.60                        |
| 2LRMRP P           | —  | 21.47                                 | 21.30                        |
| 3LRMRP P           | —  | 15.56                                 | 16.44                        |
| 3LRMRT P           | —  | 14.97                                 | 15.64                        |

Table 6 outlines the calculated and measured GR values of the GSs implemented in soil 4 (S4), for which the resistivity was 159  $\Omega$ ·m. The dry LRM (D) was used in this soil.

**Table 6.** GR calculations and measurements in S4.

| Configuration Code | Calculated Grounding Resistance ( $\Omega$ ) | Measured Grounding Resistance         |                              |
|--------------------|--|---------------------------------------|------------------------------|
|                    |  | Fall-of-Potential Method ( $\Omega$ ) | Clamp-on Method ( $\Omega$ ) |
| 1R                 | 81.57  | 93.80                                 | 93.40                        |
| 2RP                | 41.33  | 37.98                                 | 32.90                        |
| 3RP                | 27.38  | 25.04                                 | 25.70                        |
| 3RT                | 24.32  | 21.93                                 | 22.50                        |
| 1LRMR D            | —  | 62.60                                 | 44.70                        |
| 2LRMRP D           | —  | 24.18                                 | 18.86                        |
| 3LRMRP D           | —  | 17.92                                 | 17.39                        |
| 3LRMRT D           | —  | 16.50                                 | 17.82                        |

Table 7 outlines the calculated and measured GR values of the GSs implemented in soil 5 (S5), for which the resistivity was 175  $\Omega$ -m. The premixed LRM (P) was used in this soil.

**Table 7.** GR calculations and measurements in S5.

| Configuration Code | Calculated Grounding Resistance ( $\Omega$ ) | Measured Grounding Resistance         |                              |
|--------------------|--|---------------------------------------|------------------------------|
|                    |  | Fall-of-Potential Method ( $\Omega$ ) | Clamp-on Method ( $\Omega$ ) |
| 6RR                | 13.89  | 12.80                                 | 13.51                        |
| 6LRMRR P           | —  | 7.58                                  | 10.40                        |

Table 8 outlines the calculated and measured GR values of the GSs implemented in soil 6 (S6), for which the resistivity was 190  $\Omega$ -m. The dry LRM (D) was used in this soil.

**Table 8.** GR calculations and measurements in S6.

| Configuration Code | Calculated Grounding Resistance ( $\Omega$ ) | Measured Grounding Resistance         |                              |
|--------------------|--|---------------------------------------|------------------------------|
|                    |  | Fall-of-Potential Method ( $\Omega$ ) | Clamp-on Method ( $\Omega$ ) |
| 6RR                | 15.08  | 14.93                                 | 12.90                        |
| 6LRMRR D           | —  | 14.33                                 | 12.30                        |

Table 9 outlines the calculated and measured GR values of the GSs implemented in soil 7 (S7), for which the resistivity was 195  $\Omega$ -m. The premixed LRM (P) was used in this soil.

**Table 9.** GR calculations and measurements in S7.

| Configuration Code | Calculated Grounding Resistance ( $\Omega$ ) | Measured Grounding Resistance         |                              |
|--------------------|--|---------------------------------------|------------------------------|
|                    |  | Fall-of-Potential Method ( $\Omega$ ) | Clamp-on Method ( $\Omega$ ) |
| 1R                 | 100.04                                       | 96.80                                 | 95.50                        |
| 2RP                | 50.69  | 48.80                                 | 50.60                        |
| 3RP                | 33.58  | 31.70                                 | 34.10                        |
| 3RT                | 29.82  | 27.36                                 | 31.50                        |
| 1LRMR P            | —  | 53.20                                 | 43.20                        |
| 2LRMRP P           | —  | 26.58                                 | 28.20                        |
| 3LRMRP P           | —  | 21.89                                 | 20.30                        |
| 3LRMRT P           | —  | 21.01                                 | 18.90                        |

Table 10 outlines the calculated and measured GR values of the GSs implemented in soil 8 (S8), for which the resistivity was 302  $\Omega$ -m. The dry LRM (D) was used in this soil.

**Table 10.** GR calculations and measurements in S8.

| Configuration Code | Calculated Grounding Resistance ( $\Omega$ ) | Measured Grounding Resistance         |                              |
|--------------------|--|---------------------------------------|------------------------------|
|                    |  | Fall-of-Potential Method ( $\Omega$ ) | Clamp-on Method ( $\Omega$ ) |
| 1R                 | 154.94                                       | 160.9                                 | RE > 149.90                  |
| 2RP                | 78.50  | 76.30                                 | 70.90                        |
| 3RP                | 52.01  | 44.00                                 | 43.80                        |
| 3RT                | 46.19  | 42.80                                 | 42.20                        |

Table 10. Cont.

| Configuration Code | Calculated Grounding Resistance ( $\Omega$ ) | Measured Grounding Resistance Fall-of-Potential Method ( $\Omega$ ) | Measured Grounding Resistance Clamp-on Method ( $\Omega$ ) |
|--------------------|--|---|--|
| 1LRMR D            | —  | 31.26   | 33.34  |
| 2LRMRP D           | —  | 15.73   | 15.46  |
| 3LRMRP D           | —  | 12.23   | 12.50  |
| 3LRMRT D           | —  | 12.18   | 12.14  |

### 5. Analysis of the Results

#### 5.1. LRM Effects on Soils with Different Resistivity Values

Figures 8–12 show the effect of the soil resistivity on the GR when the vertical rods of each GS design were covered with the LRMs. The results show that the ground resistivity increased as the GR of the LRM decreased.

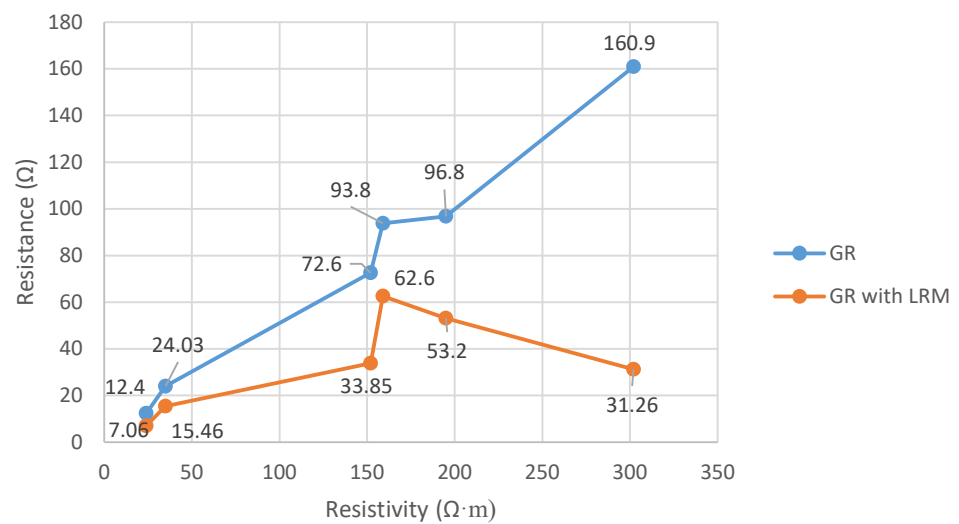


Figure 8. GR vs. 1R resistivity.

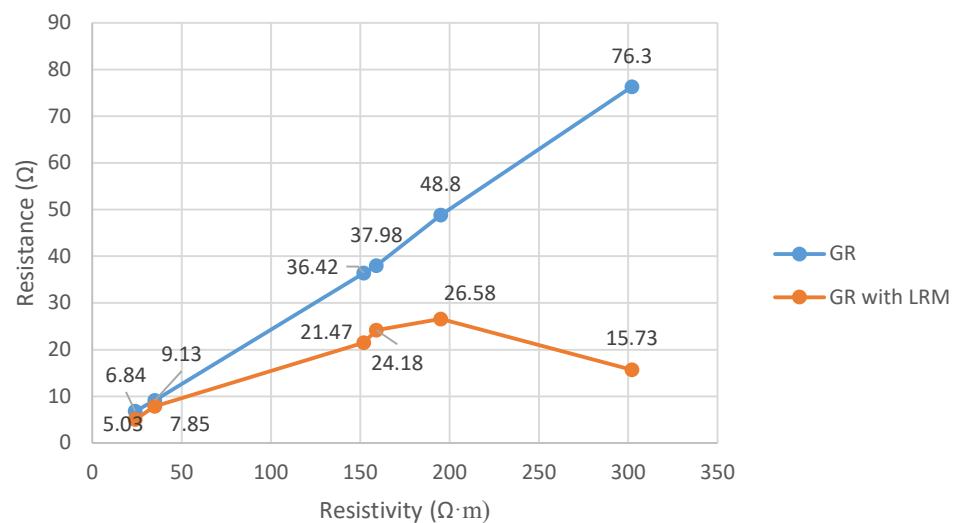


Figure 9. GR vs. 2RP resistivity.

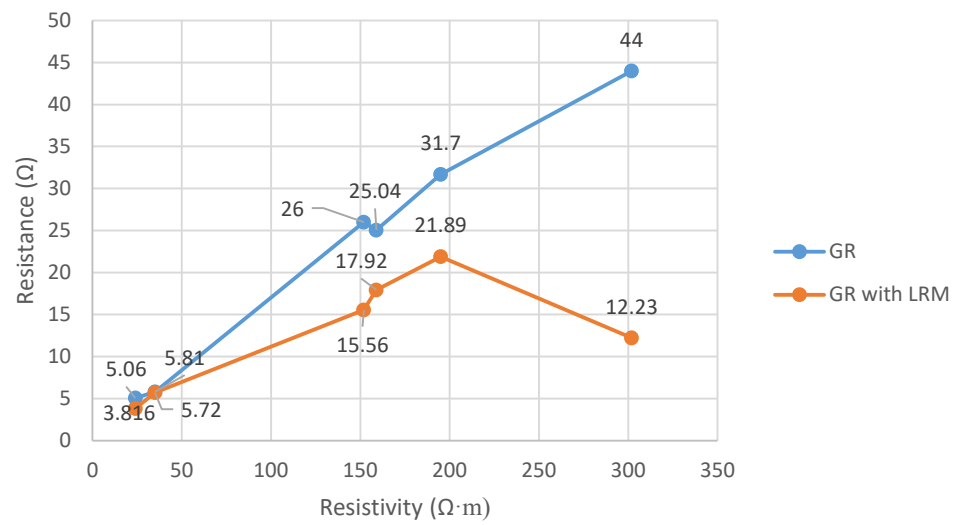


Figure 10. GR vs. 3RP resistivity.

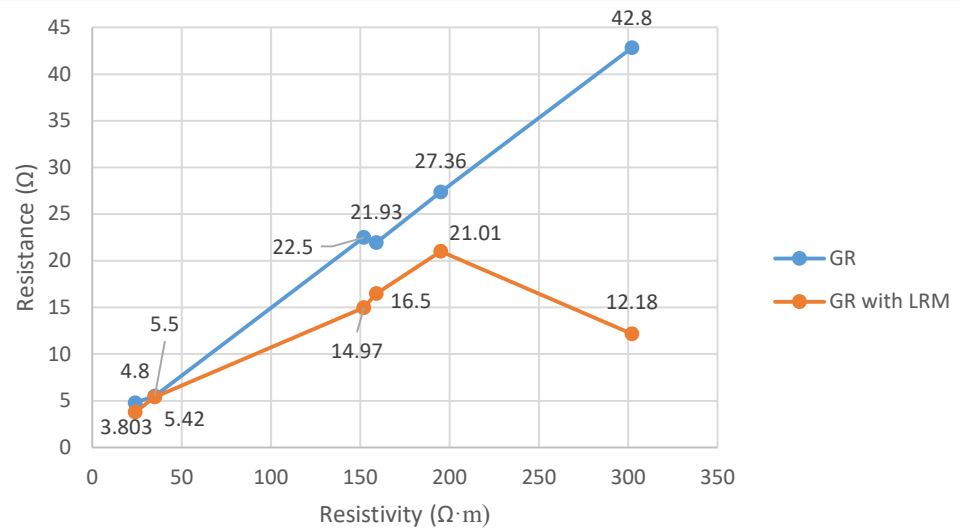


Figure 11. GR vs. 3RT resistivity.

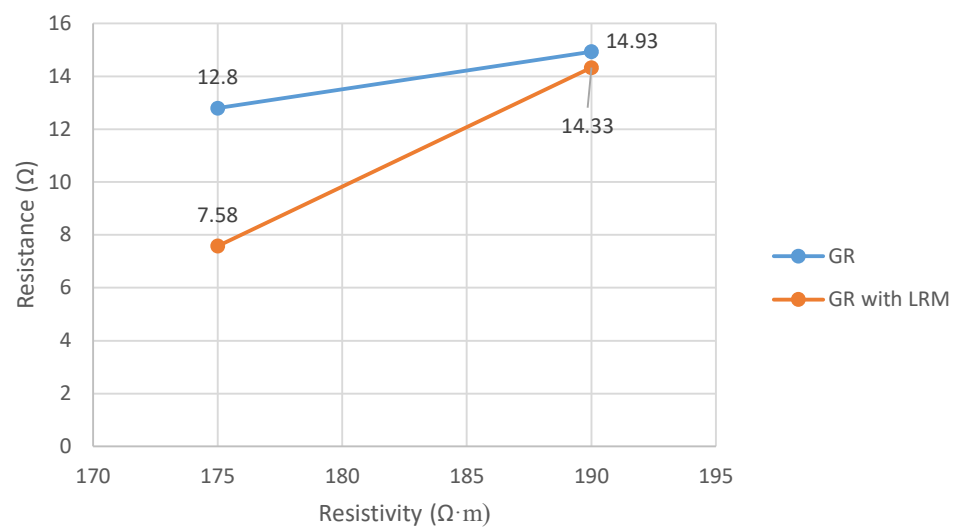


Figure 12. GR vs. 6RR resistivity.

In the one-rod GS designs with an LRM (1LRMR), the GR reduction ranged from the original value to 5.34 Ω (43%) in low-resistivity soils such as S1, with a resistivity of 24 Ω·m, to 129.64 Ω (81%) in high-resistivity soils such as S8, with a resistivity of 302 Ω·m.

For a more complex design than the previous case, as in the triangular grid configuration with an LRM (3LRMRT), the GR reduction ranged from its original value of 1.00 Ω (21%) in low-resistivity soils such as S1, with a resistivity of 24 Ω·m, to 30.62 Ω (72%) in high-resistivity soils such as S8, with a resistivity of 302 Ω·m.

In each design, the GR of the LRM (ΔGR) decreased as the soil resistivity increased, as shown in the columns of Table 11. In this study, the vertical rods were covered with premixed (P) and dry (D) LRMs.

Table 11. Summary of the results of the LRM effect.

| S | ρ (Ω·m) | LRM | 1LRMR   |         | 2LRMRP  |         | 3LRMRP  |         | 3LRMRT  |         | 6LRMRR  |         |
|---|---------|-----|---------|---------|---------|---------|---------|---------|---------|---------|---------|---------|
|   |         |     | ΔGR (Ω) | ΔGR (%) |
| 1 | 24      | P   | 5.34    | 43%     | 1.81    | 26%     | 1.24    | 25%     | 1.00    | 21%     | —       | —       |
| 2 | 35      | D   | 8.57    | 36%     | 1.28    | 14%     | 0.09    | 2%      | 0.08    | 1%      | —       | —       |
| 3 | 152     | P   | 38.75   | 53%     | 14.95   | 41%     | 10.44   | 40%     | 7.53    | 33%     | —       | —       |
| 4 | 159     | D   | 31.20   | 33%     | 13.80   | 36%     | 7.12    | 28%     | 5.43    | 25%     | —       | —       |
| 5 | 175     | P   | —       | —       | —       | —       | —       | —       | —       | —       | 5.22    | 41%     |
| 6 | 190     | D   | —       | —       | —       | —       | —       | —       | —       | —       | 0.60    | 4%      |
| 7 | 195     | P   | 43.60   | 45%     | 22.22   | 46%     | 9.81    | 31%     | 6.35    | 23%     | —       | —       |
| 8 | 302     | D   | 129.64  | 81%     | 60.57   | 79%     | 31.77   | 72%     | 30.62   | 72%     | —       | —       |

P = Premixed. D = Dry.

As shown above, as the higher ground resistivity increased, the GR of the LRM decreased. As previously mentioned, the climatic conditions varied during this project. If new readings are taken during the winter season, the GR should decrease; in contrast, if measurements are taken in the summer, the GR should increase. Similarly, no single trend in the change in the GR was observed because two types of LRMs were used in this study.

5.2. LRM Effect as a Function of GS Design

Figures 13–18 and Table 11 show the variations in the GR (ΔGR) for the LRMs as the design complexity of the GS increased.

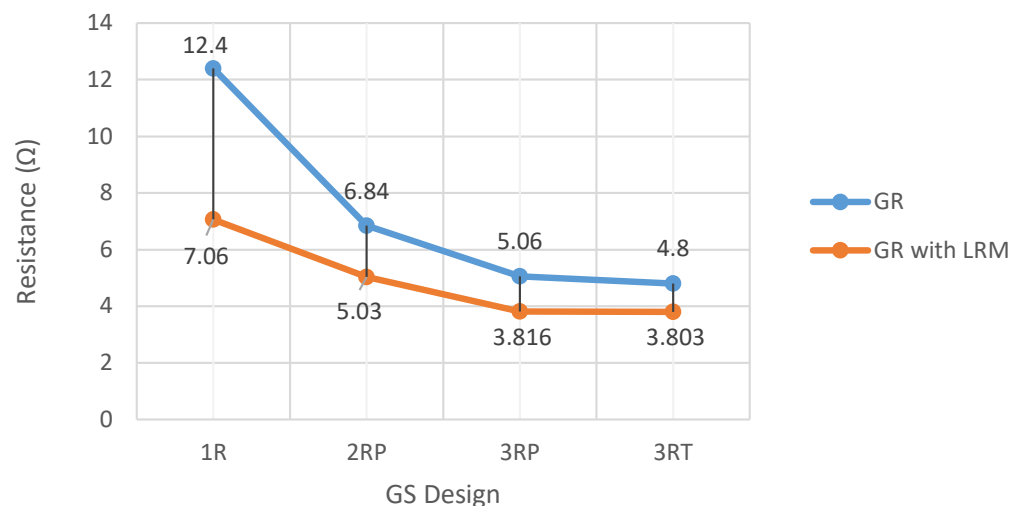


Figure 13. GR vs. GS design in S1.

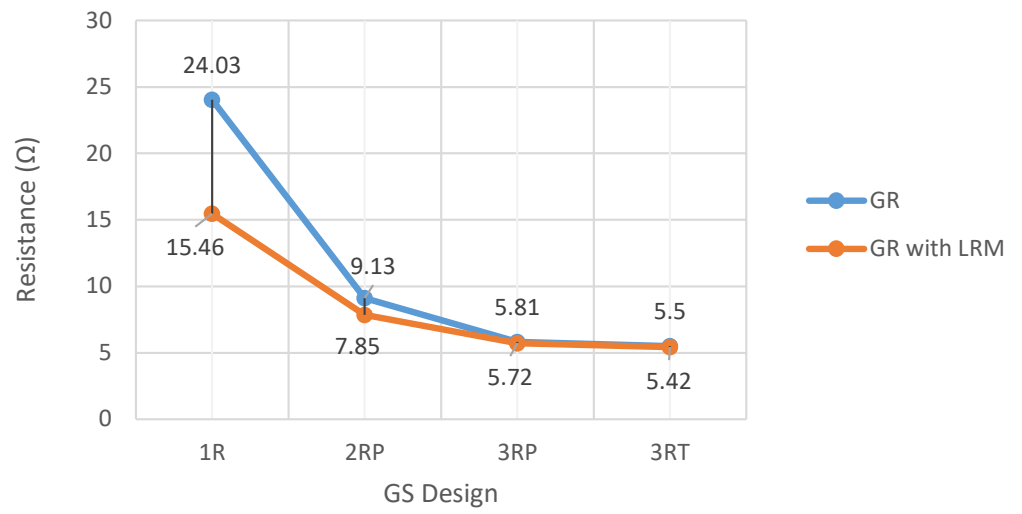


Figure 14. GR vs. GS design in S2.

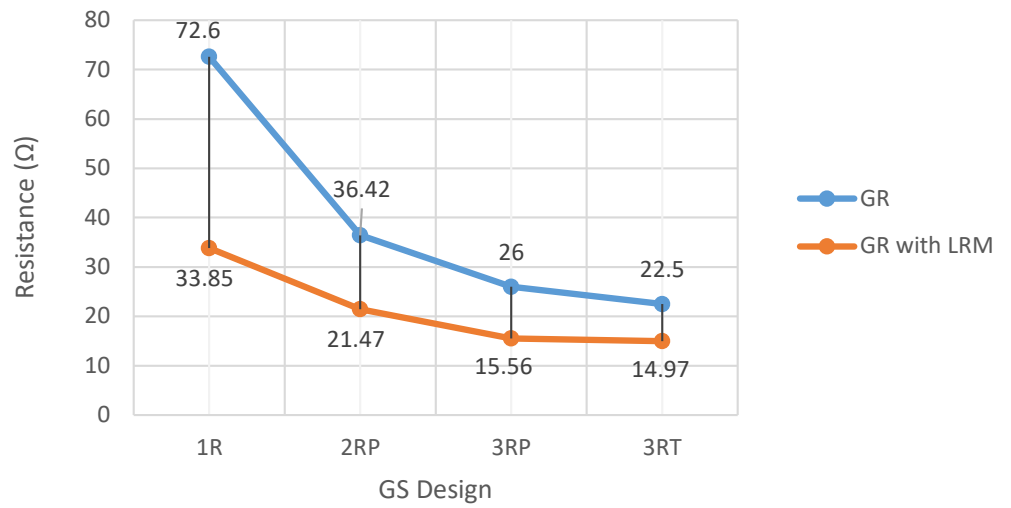


Figure 15. GR vs. GS design in S3.

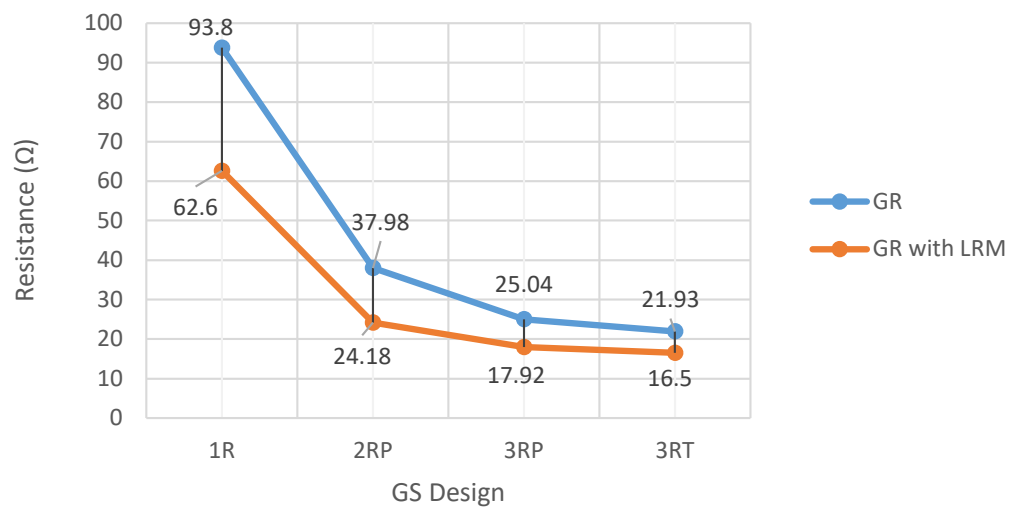


Figure 16. GR vs. GS design in S4.

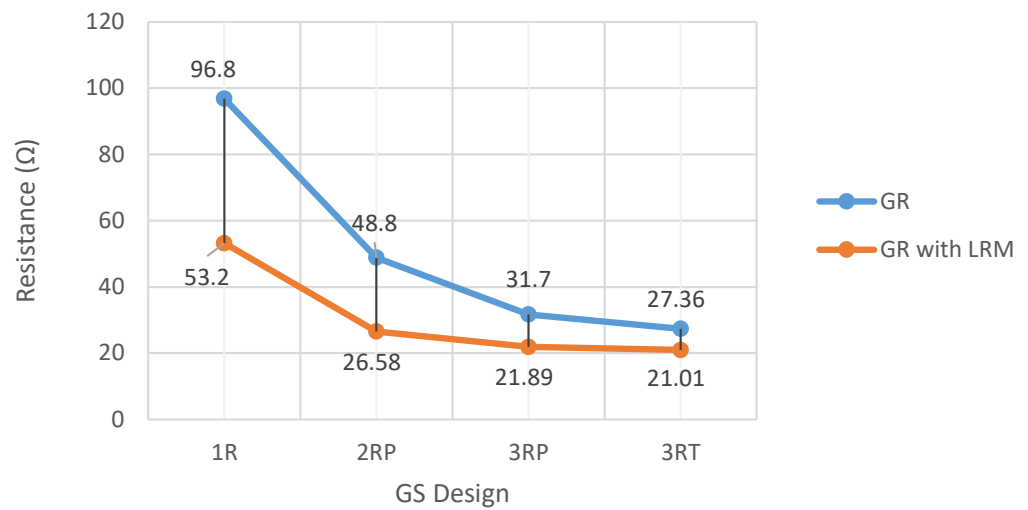


Figure 17. GR vs. GS design in S7.

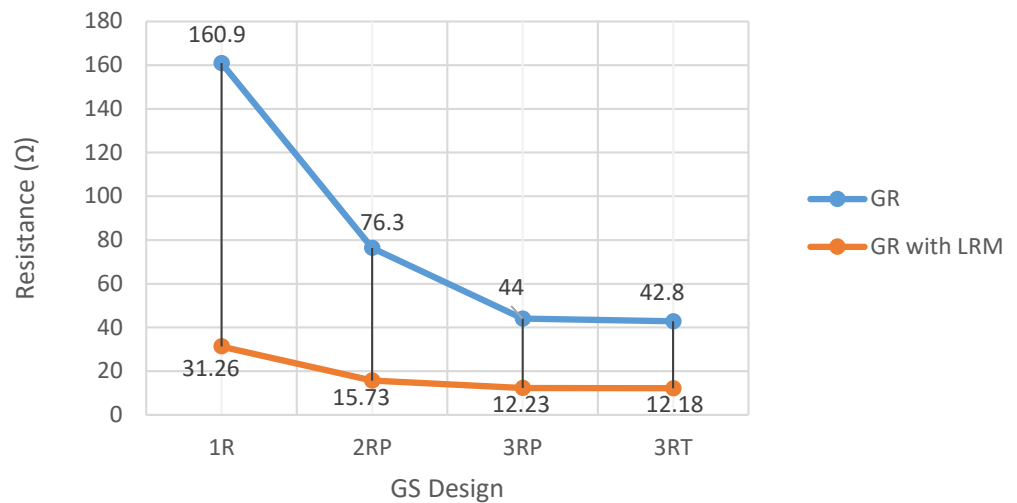


Figure 18. GR vs. GS design in S8.

These results show that, for example, in the one-rod design with an LRM (1LRMR) in a low-resistivity soil such as S1, with a resistivity of 24 Ω·m, the GR decreased from its original value to 5.34 Ω (43%). In contrast, in the triangular grid design with an LRM (3LRMRT) in the same soil, the GR decreased to 1 Ω (21%).

In a high-resistivity soil such as S8, with a resistivity of 302 Ω·m, the GR decreased from its original value in the one-rod design with an LRM (1LRMR) to 129.64 Ω (81%), whereas for the 3LRMRT design in the same soil, the GR decreased to 30.62 Ω (72%).

Thus, as the complexity of the GS design increased, the reduction in the GR of the LRM decreased.

In addition, the LRM effect was assessed on two rectangular grids of six-rod GSs. One grid was placed in soil 5 (S5), with a resistivity of 175 Ω·m, with the premixed LRM covering each of the vertical rods, and the GR decreased from its original value of 5.22 Ω. The other grid was placed in soil 6 (S6), with a resistivity of 190 Ω·m, with the dry LRM covering each of the vertical rods, and the GR decreased to 0.60 Ω. A considerable GR reduction was not obtained despite the high resistivity of the soil because the GS design was even more complex.

### 5.3. Ranges of LRM GR Variation

To estimate the range of the decrease in the GR of the LRMs, the premixed and dry LRM results were first combined to complement the values with conservative percentages, as shown in Table 12; that is, when the LRMs were used, the GR was reduced by a larger percentage. In addition, the effect of the LRMs did not follow a linear or logarithmic relationship with the resistivity or the GS design. Similarly, different LRMs (types and brands) were used.

**Table 12.** LRM GR reduction by ground resistivity and GS design.

| $\rho$ ( $\Omega\cdot\text{m}$ ) | 1LRMR           | 2LRMRP          | 3LRMRP          | 3LRMRT          | 4LRMRS          | 6LRMRR          |
|----------------------------------|-----------------|-----------------|-----------------|-----------------|-----------------|-----------------|
|                                  | $\Delta$ GR (%) |
| 1–10                             | 30%             | 21%             | 16%             | 13%             | 12%             | 11%             |
| 11–20                            | 37%             | 28%             | 25%             | 21%             | 19%             | 18%             |
| 21–30                            | 40%             | 28%             | 25%             | 21%             | 19%             | 18%             |
| 31–40                            | 40%             | 28%             | 25%             | 21%             | 19%             | 18%             |
| 41–50                            | 40%             | 28%             | 25%             | 21%             | 19%             | 18%             |
| 51–60                            | 40%             | 28%             | 25%             | 23%             | 22%             | 25%             |
| 61–70                            | 40%             | 28%             | 25%             | 23%             | 22%             | 25%             |
| 71–80                            | 40%             | 28%             | 25%             | 23%             | 22%             | 25%             |
| 81–90                            | 40%             | 28%             | 25%             | 23%             | 22%             | 25%             |
| 91–100                           | 40%             | 28%             | 25%             | 28%             | 27%             | 25%             |
| 101–110                          | 40%             | 40%             | 38%             | 28%             | 27%             | 25%             |
| 111–120                          | 50%             | 40%             | 38%             | 33%             | 29%             | 27%             |
| 121–130                          | 50%             | 40%             | 38%             | 33%             | 29%             | 27%             |
| 131–140                          | 50%             | 40%             | 38%             | 33%             | 29%             | 27%             |
| 141–150                          | 50%             | 40%             | 38%             | 33%             | 29%             | 27%             |
| 151–160                          | 50%             | 40%             | 38%             | 33%             | 29%             | 27%             |
| 161–170                          | 50%             | 40%             | 38%             | 33%             | 29%             | 27%             |
| 171–180                          | 50%             | 46%             | 38%             | 36%             | 33%             | 30%             |
| 181–190                          | 50%             | 46%             | 38%             | 36%             | 33%             | 30%             |
| 191–200                          | 50%             | 46%             | 38%             | 36%             | 33%             | 30%             |
| 201–210                          | 50%             | 46%             | 40%             | 38%             | 36%             | 30%             |
| 211–220                          | 55%             | 50%             | 40%             | 38%             | 36%             | 30%             |
| 221–230                          | 55%             | 50%             | 45%             | 40%             | 36%             | 30%             |
| 231–240                          | 60%             | 55%             | 50%             | 45%             | 40%             | 33%             |
| 241–250                          | 60%             | 55%             | 50%             | 45%             | 40%             | 33%             |

Table 12 outlines the range of reduction in the GR value when the 1.8-m vertical rods were covered with the LRMs and a #2 AWG bare grounding wire was used. For example, the one-rod GS design covered with an LRM (1LRMV) showed a 30% reduction in the GR value in soils with resistivities ranging from 1 to 10  $\Omega\cdot\text{m}$  and a 60% reduction in soils with resistivities ranging from 241 to 250  $\Omega\cdot\text{m}$ .

When the 1.8-m rods were placed in the soil with a resistivity of 10  $\Omega\cdot\text{m}$ , the GR was 5.13  $\Omega$ ; when the rods were covered with the LRMs, the GR decreased by 1.54  $\Omega$  or 30% to 3.59  $\Omega$ . In turn, when the 1.8-m rods were placed in the soil with a resistivity of 250  $\Omega\cdot\text{m}$ ,

the GR was 128.26  $\Omega$ ; when the rods were covered with an LRM, the GR decreased by 76.96  $\Omega$  or 60% to 51.30  $\Omega$ .

## 6. Discussion

In this study, various GS configurations were implemented (see Figure 1). These configurations were chosen mainly because they make it possible to compare measured GR values with calculated GR values. Such a comparison is very useful because the GR performance can be assessed by installing LRMs in each of the vertical rods. In the literature there are field tests applying LRM in different configurations, but on a reduced scale, where the GR results could not be related to the existing formulation when another type of grounding mesh is required, even more so when it is required calculate the GR by modifying the formulation variables (see the formulation and its respective variables in Section 3.4); for example, Ref. [30] installed a 2 m  $\times$  2 m grid in three soils with different resistivities. Ref. [31] installed five individual rods in each of five soils with different resistivities, and Ref. [32] used three cylindrical rods with the same length ( $l = 50$  cm) but different diameters.

In the present study, the results show that as the soil resistivity increased, the decrease in the GR of the LRMs decreased. This correlation matches the results of other studies, such as [14,17,33], which reported different GR reduction percentages because each study used different LRMs, GS designs and soil resistivities. Likewise in [20] showed that using an LRM with a 2.4-m ground rod reduced the GR by approximately 40% when the resistivity of the surrounding soil was higher than 250  $\Omega$ -m and by approximately 50% when the resistivity of the surrounding soil was higher than 300  $\Omega$ -m. Conversely, in this study, the results show that the GR of the LRMs for the 1.8-m rod decreased by 45% when the resistivity of the surrounding soil was 195  $\Omega$ -m and by 81% when the resistivity of the surrounding soil was 302  $\Omega$ -m. In [34] the GR decrease with LRM on average is 42.05% and in [35] the LRM reduction is 20% for a 3 m vertical rod in a 103.6  $\Omega$ -m soil from the nearest layer.

As mentioned above, most LRM studies are isolated and small-scale, that is, they present results for a single configuration, in a single field of a given resistivity, and do not relate the results to the theoretical calculation. Single GR reduction percentages with LRM may confuse the reader, implying that these percentages are given for any configuration and in any soil of different resistivity. On the other hand, this study presents different configurations, terrains with different resistivity values, relationship with the theoretical calculation, and above all, field tests and measurements are carried out; resulting in different values of GR reduction (see Table 12).

## 7. Conclusions

The soil resistivity value is a key requirement for GS designs. Although some tables of the relationship between the type of soil and its resistivity, geological maps and graphs from which general resistivity ranges can be determined are available in the literature, the resistivity must be measured in the location where the components of a GS are to be installed.

LRMs were installed in each of the vertical rods of the designs studied here (see Figure 4) to assess how they affected the GR as a function of both the GS design and the ground resistivity. Premixed and dry LRMs were used, considering the variations in costs, building methods and compactness. The GR of the LRMs was measured using the three aforementioned methods 28 days after installation due to the contact between the rods (including the LRM) and the ground.

The results show that the GR of the LRM markedly decreased in the high-resistivity soils. Conversely, in the low-resistivity soils, no significant changes occurred. Similarly, the LRMs showed a better effect for the simple GS designs, such as the one-rod (1R) design, than for the complex GS designs, such as the rectangular grid of six vertical rods (6RR) (see Table 11).

This article presents the most important results from the experimental plots in eight locations, each of which contained several GS designs with LRMs in both low- (such as S1 with a resistivity of  $24 \Omega\cdot\text{m}$ ), and high-resistivity (such as S8 with a resistivity of  $302 \Omega\cdot\text{m}$ ) soils. Practical aspects of the application of standard procedures in GS engineering are presented: application of the Wenner method, soil interpretation using the results from the Wenner method, GR calculation of the designed GSs and GR measurements. Experimental studies on the effects of LRMs are generally based on laboratory and/or small-scale tests.

The main findings of this study, which was based on a combination of calculations and measurements and the use of LRMs, are presented in Table 12. This table outlines the percentage values of the reduction in the GR when the LRMs were used compared to the original values. These percentages varied for the GS design and the ground resistivity.

Through the formulation of Section 3.4, the GR can be calculated by modifying the different variables involved, and later, depending on the design chosen, apply the reduction percentage when LRM is applied to the vertical rods. Thus obtaining the calculation and design of the grounding mesh with LRM; the higher the resistivity, the greater the number of rods and conductor wire can be reduced. Although it is true that Table 12 is limited to  $250 \Omega\cdot\text{m}$ , the study can be extended to soils with higher resistivity, achieving a greater percentage reduction in GR, and above all relating the grounding configurations land with the theoretical calculation. Likewise, additional studies could be carried out by implementing LRM in the conductor cable buried horizontally, taking into account that this would require significant financing.

The entire study was conducted following guidelines and recommendations, primarily IEEE standard 80-2013 [3] and IEEE standard 81-2012 [26]. Electrical engineers, electricians, researchers, and people associated with the area of earth leakage protection can easily use the results from this study to design GSs according to the required GR, either using common materials or LRMs.

**Author Contributions:** Conceptualization, A.B.-E.; Data curation, A.B.-E. and F.Q.-P.; Funding acquisition, A.B.-E. and F.Q.-P.; Investigation, F.S.-S.; Methodology, F.S.-S. and C.C.-N.; Project administration, A.B.-E.; Resources, F.Q.-P.; Software, F.S.-S. and C.C.-N.; Supervision, A.B.-E.; Validation, F.S.-S. and C.C.-N.; Visualization, F.Q.-P.; Writing—original draft, F.S.-S.; Writing—review & editing, A.B.-E. All authors have read and agreed to the published version of the manuscript.

**Funding:** This research was funded by the Energy Research Group (GIE) of the Salesian Polytechnic University, Cuenca, Ecuador under resolution N° 003-005-2019-07-18.

**Institutional Review Board Statement:** Not applicable.

**Informed Consent Statement:** Not applicable.

**Data Availability Statement:** The data supporting the results reported in this study can be found at the following handle: <http://dspace.ups.edu.ec/handle/123456789/20439> (accessed on 3 May 2022).

**Acknowledgments:** The authors wish to express their most sincere acknowledgement and gratitude to the Salesian Polytechnic University (Universidad Politécnica Salesiana—UPS), particularly the Energy Research Group (GIE), for their guidance and for funding this research.

**Conflicts of Interest:** The authors declare no conflict of interest.

## References

1. Androvitsaneas, V.P.; Gonos, I.F.; Stathopoulos, I.A. Research and applications of ground enhancing compounds in grounding systems. *IET Gener. Transm. Distrib.* **2017**, *11*, 3195–3201. [[CrossRef](#)]
2. Montaña, J. *Teoría de Puestas a Tierra*, 1st ed.; Editorial Universidad del Norte: Barranquilla, Colombia, 2011.
3. *IEEE Std 80-2013 (Revision of IEEE Std 80-2000/ Incorporates IEEE Std 80-2013/Cor 1-2015)*; IEEE Guide for Safety in AC Substation Grounding; IEEE: Piscataway, NJ, USA, 2015; pp. 1–226.
4. Al-Arainy, A.A.; Khan, Y.; Qureshi, M.I.; Malik, N.H.; Pazheri, F.R. Optimized pit configuration for efficient grounding of the power system in high resistivity soils using low resistivity materials. In Proceedings of the 2011 Fourth International Conference on Modeling, Simulation and Applied Optimization, Kuala Lumpur, Malaysia, 19–21 April 2011; pp. 1–5. [[CrossRef](#)]

5. Sinchi, F.M.; Quizhpi, F.A.; Guillén, H.P.; Quinde, S.N. Soil Treatment to Reduce Grounding Resistance by Applying Low-Resistivity Material (LRM) and Chemical Ground Electrode in Different Grounding Systems Configurations. In Proceedings of the 2018 IEEE International Autumn Meeting on Power, Electronics and Computing (ROPEC), Ixtapa, Mexico, 14–16 November 2018; pp. 1–6.
6. Sengar, K.P.; Chandrasekaran, K. Comparative Analysis of Grounding Grid Configurations with Equal and Unequal Spaced Design. In Proceedings of the 2019 IEEE 1st International Conference on Energy, Systems and Information Processing (ICESIP), Chennai, India, 4–6 July 2019; pp. 1–6.
7. He, J.; Zeng, R.; Zhang, B. *Methodology and Technology for Power System Grounding*; John Wiley & Sons Singapore Pte. Ltd.: Singapore, 2012. [CrossRef]
8. Reynolds, J.M. *An Introduction to Applied and Environmental Geophysics*, 2nd ed.; Wiley-Blackwell: Hoboken, NJ, USA, 2011; p. 710.
9. Gilbert, G. High Voltage Grounding Systems. Ph.D. Thesis, University of Waterloo, Waterloo, ON, Canada, 2011.
10. UNE-EN 50522; Puesta a Tierra en Instalaciones de Tensión Superior a 1 kV en Corriente Alterna. Aenor Norma Española: Madrid, Spain, 2012; p. 71.
11. Sinchi, F.; Guillén, H. Diseño y Determinación de Sistemas de Puesta a Tierra Mediante Pruebas de Campo con Elementos Comunes Utilizados en la Región, Incluyendo GEM y Electrodo Químico. Ph.D. Thesis, Universidad Politécnica Salesiana, Cuenca, Ecuador, 2017. Available online: <http://dspace.ups.edu.ec/handle/123456789/14487> (accessed on 21 February 2022).
12. Lai, W.L.; Ahmad, W.F.H.W.; Jasni, J.; Ab Kadir, M.Z.A. A review on the usage of Zeolite, Perlite and Vermiculite as natural enhancement materials for grounding system installations. In Proceedings of the 2017 IEEE 15th Student Conference on Research and Development (SCORED), Wilayah Persekutuan Putrajaya, Malaysia, 13–14 December 2017; pp. 338–343.
13. Eduful, G.; Cole, J.E.; Okyere, P. Optimum mix of ground electrodes and conductive backfills to achieve a low ground resistance. In Proceedings of the 2009 2nd International Conference on Adaptive Science & Technology (ICAST), Accra, Ghana, 14–16 January 2009; pp. 140–145. [CrossRef]
14. Prabhakar, C.; Deshpande, R.A. Evaluation of soil resistivity and design of grounding system for hydroelectric generating station in a hilly terrain—A case study. In Proceedings of the 2014 International Conference on Advances in Energy Conversion Technologies (ICAECT), Manipal, India, 23–25 January 2014; pp. 104–107.
15. Jones, W. Bentonite Rods Assure Ground Rod Installation In Problem Soils. *IEEE Trans. Power Appar. Syst.* **1980**, PAS-99, 1343–1346. [CrossRef]
16. Khan, Y.; Malik, N.H.; Al-Arainy, A.A.; Qureshi, M.I.; Pazheri, F.R. Efficient use of low resistivity material for grounding resistance reduction in high soil resistivity areas. In Proceedings of the TENCON 2010—2010 IEEE Region 10 Conference, Fukuoka, Japan, 21–24 November 2010; pp. 620–624. [CrossRef]
17. Youping Tu.; Jinliang He.; Rong Zeng. Lightning impulse performances of grounding devices covered with low-resistivity materials. *IEEE Trans. Power Deliv.* **2006**, 21, 1706–1713. [CrossRef]
18. Kostic, M.; Radakovic, Z.; Radovanovic, N.; Tomasevic-Canovic, M. Improvement of electrical properties of grounding loops by using bentonite and waste drilling mud. *IEE Proc.-Gener. Transm. Distrib.* **1999**, 146, 1. [CrossRef]
19. Androvitsaneas, V.P.; Asimakopoulou, F.E.; Gonos, I.F.; Stathopoulos, I.A. Estimation of ground enhancing compound performance using Artificial Neural Network. In Proceedings of the 2012 International Conference on High Voltage Engineering and Application, Shanghai, China, 17–20 September 2012; pp. 145–149. [CrossRef]
20. Al-Ammar, E.; Khan, Y.; Malik, N.; Wani, N. Development of low resistivity material for grounding resistance reduction. In Proceedings of the 2010 IEEE International Energy Conference, Manama, Bahrain, 18–22 December 2010; pp. 700–703. [CrossRef]
21. Hidalgo, N.; Senese, A.; Cano, E.; Sarquís, P. Caracterización y evaluación de la calidad de bentonitas provenientes de las provincias de San Juan y Río Negro (Argentina) para uso en industria petrolera y cerámica. *Bol. Geol. Min.* **2016**, 127, 791–806. [CrossRef]
22. Tapia, M.E.F. The Ineffectiveness of the Bond Issued in Favor of the Federal Treasury. Chapter 1. Research Project. 2004. Available online: [http://catarina.udlap.mx/u\\$\\_\\$dl\\$\\_\\$\\_\\$/tales/documentos/ledf/flores\\$\\_\\$\\_\\$t\\$\\_\\$\\_\\$me/](http://catarina.udlap.mx/u$_$dl$_$_$/tales/documentos/ledf/flores$_$_$t$_$_$me/) (accessed on 10 January 2022).
23. Francry Maigualida. Métodos de Recolección de Datos. Ph.D. Thesis, Universidad de Carabobo, Valencia, Spain, 2004.
24. Dwight, H.B. Calculation of Resistances to Ground. *Trans. Am. Inst. Electr. Eng.* **1936**, 55, 1319–1328. [CrossRef]
25. Sinchi, F.M.; Quizhpi, F.A.; Guillén, H.P. Calculation of the earth resistance of the union of two and three rods by modified Schwarz equations and field tests. In Proceedings of the 2017 IEEE International Autumn Meeting on Power, Electronics and Computing (ROPEC), Ixtapa, Mexico, 8–10 November 2017; pp. 1–6.
26. *IEEE Std 81-2012 (Revision of IEEE Std 81-1983)—Redline*; IEEE Guide for Measuring Earth Resistivity, Ground Impedance, and Earth Surface Potentials of a Grounding System—Redline; IEEE: Piscataway, NJ, USA, 2012; pp. 1–192.
27. Alvaro, J.; Uvidia, C. Comportamiento de la Resistividad Eléctrica de los Suelos ante Variaciones de Humedad y Grado de Compactación. Ph.D. Thesis, Universidad de Cuenca, Cuenca, Ecuador, 2015.
28. Pacheco, Á.; Jiménez, J.; Quizhpi, F. Diseño De Sistemas De Puesta a Tierra Partiendo De Un Modelo Biestratificado De Terreno, Aplicando Un Software Computacional En El Sector Industrial. Ph.D. Thesis, Universidad Politécnica Salesiana, Cuenca, Ecuador, 2013.
29. Barros, H.; Ortega, L. Análisis y Diseño de la Instalación Eléctrica de una Electrolinera en la Ciudad de Cuenca. Ph.D. Thesis, Universidad Politécnica Salesiana, Cuenca, Ecuador, 2018.

30. Reffin, M.S.; Nor, N.M.; Abdullah, S.; Ahmad, N.; Othman, M. Impulse Characteristics of Earth Electrodes in Different Soil Resistivity by Field Measurements. In Proceedings of the 2018 IEEE PES Asia-Pacific Power and Energy Engineering Conference (APPEEC), Kota Kinabalu, Malaysia, 7–10 October 2018; pp. 331–334. [[CrossRef](#)]
31. Choun, L.W.; Gomes, C.; Ab, Kadir, M.Z.; Ahmad, W.F. Analysis of earth resistance of electrodes and soil resistivity at different environments. In Proceedings of the 2012 International Conference on Lightning Protection (ICLP), Vienna, Austria, 2–7 September 2012; pp. 1–9. [[CrossRef](#)]
32. Rio, H.D.; Bambang, A.S. Characteristic study of vertical configuration grounding system with two layer modified using type of different soil for variation of diameter and frequency injection. In Proceedings of the 2nd IEEE Conference on Power Engineering and Renewable Energy (ICPERE) 2014, Bali, Indonesia, 9–11 December 2014; pp. 214–219. [[CrossRef](#)]
33. Wan Ahmad, W.F.H.; Lai, W.L.; Jasni, J.; Ab-Kadir, M.Z.A. Variations of Soil Resistivity Values due to Grounding System Installations with Natural Enhancement Material Mixtures. In Proceedings of the 2018 34th International Conference on Lightning Protection (ICLP), Rzeszow, Poland, 2–7 September 2018; pp. 1–5. [[CrossRef](#)]
34. Wan Ahmad, W.F.H.; Hamzah, N.H.; Jasni, J.; Ab-Kadir, M.Z.A.; Gomes, C. A Study on Bentonite and Kenaf Properties for Grounding Purposes. In Proceedings of the 2018 34th International Conference on Lightning Protection (ICLP), Rzeszow, Poland, 2–7 September 2018; pp. 1–8. [[CrossRef](#)]
35. Ahmad, S.K.; Sabry, R.Z.; Gomes, C. Improving the Grounding System by Adding Bentonite to Reduce the Potential Distribution. In Proceedings of the 2021 International Conference on Electrical, Communication, and Computer Engineering (ICECCE), Kuala Lumpur, Malaysia, 12–13 June 2021; pp. 1–5. [[CrossRef](#)]